Research Article

Characterization of a hypersporulating strain derivative *of Clostridioides difficile* R20291

Francisca Cid-Rojas[1], Daniel Paredes-Sabja[1,*]

[1]Department of Biology, Texas A&M University, College Station, Texas, USA

Running Title: Characterization of a hypersporulating derivative of *Clostridioides difficile* R20291 strain

Key Words: *C. difficile* spores, hypersporulation, sporulation, R20291, exosporium, spore coat, *rsbV*.

*Corresponding Author. Dr. Daniel Paredes-Sabja, Department of Biology, Texas A&M University, College Station, TX, 77843, USA. E-mail: dparedes-sabja@bio.tamu.edu

Abstract

Clostridioides difficile is a Gram-positive and obligate anaerobic spore-former pathogen. *C. difficile* spores are essential for the transmission and recurrence of *C. difficile* infections (CDI). A major challenge in sporulation studies in *C. difficile* is the low yield and asynchronous nature of this process. In this work, a hypersporulating strain, derivative of R20291, with an early sporulation onset and enhanced sporulation efficiency was isolated by serendipity. This strain had 1000-fold higher sporulation efficiency than the parental R20291 strain in sessile culture conditions. Electron micrographs revealed that spores of both strains have similar hair-like projections, electron-dense outer exosporium layer features. Whole genome sequencing and genomic analyses revealed that the hypersporulating strain had a 2356 bp-deletion spanning three ORF, including a non-essential *proC1* involved in proline metabolism, and a missense mutation in *rsbV*, an anti-anti-SigB factor of RsbW. These observations suggest that this RsbV-variant might contribute to constitutive repression of the SigB-dependent general stress response, and therefore, derepressing sporulation in this hypersporulating strain.

Introduction

Clostridioides difficile is an anaerobic, Gram-positive, spore-forming pathogen and the principal etiologic agent of *C. difficile* infection (CDI), as well as, currently being the most frequent healthcare-associated cause of infectious diarrhea in industrialized countries (1, 2). CDI typically occurs after antibiotic-mediated disruption of the normal gut microbiota, enabling endogenous or ingested *C. difficile* spores to germinate and colonize (3, 4). Clinical manifestations range from mild diarrhea to pseudomembranous colitis, toxic megacolon and, in severe cases, death (3, 4). Moreover, recurrent CDI (R-CDI) remains a major public-health challenge, which affects 20-30% of CDI patients and may increase to nearly 60% after multiple episodes (5, 6).

The infection cycle of *C. difficile* is primarily driven by its ability to produce metabolically dormant and environmentally resilient spores (7). After ingestion, spores survive the passage through the stomach and germinate in the gastrointestinal tract in response to bile acids and other cues (7, 8), leading to colonization, toxin production, and disease development (9). A subset of cells initiate sporulation, generating new spores that can persist in the host and are shed into the environment (10).

Although the core regulatory stages of sporulation have been characterized in *C. difficile*, sporulation-related studies are challenging due to low sporulation frequency under laboratory conditions (11-14), and that cultures undergo sporulation in an inherently asynchronous manner (12, 15). Unlike other genetically trackable spore-formers, such as *B. subtilis* and *C. perfringens*, the heterogeneity and low sporulation frequency in *C. difficile*,

complicates detailed investigations of sporulation-specific phenotypes, limits the ability to obtain stage-enriched populations, and reduces yields of purified spores for biochemical, structural, or high-throughput assays. Attempts to create high sporulating strains in *C. difficile* have met partial success, such as overexpression of Spo0A (11), however, tunning sporulation commitment requires consideration of additional regulators such as the phosphatase Spo0E and RtsA, both known to act as repressors by sequestering Spo0A (16, 17).

In the context of unrelated culturing of *C. difficile*, we serendipitously identified a derivative of the epidemic lineage strain R20291 that exhibits a distinguishable hypersporulation phenotype. In this study, we characterize this hypersporulating strain ($R20291_{CM196}$) and assess its potential as a laboratory tool for generating high-yield and more synchronous spore preparations. We observed that $R20291_{CM196}$ presented a 30 to 1,000-fold increase in ethanol-resistant CFU, depending on the sporulation media composition, and reached a total of ~ 60 % sporulating cells after 24 h of incubation in 70:30 agar plates. Moreover, electron micrographs show that spores from the hypersporulating strain are identical to parental strain. Whole genome sequence revealed the presence of a ~2000 bp deletion including a pyrroline-carboxylate reductase, *proC1*, involved in proline biosynthesis and a single nucleotide polymorphism in *rsbV*, an anti-anti-SigB factor, involved in the general stress response and inhibition of sporulation by Spo0E activation. Because this sporulation phenotype occurs under *in vitro* conditions, the strain offers a practical platform for detailed studies of *C. difficile* sporulation and spore physiology, where higher frequency of individual developmental stages is required.

Materials and Methods

Bacterial strains and growth conditions

C. difficile strains were routinely grown at 37 °C under anaerobic conditions in a Coy Vinyl Anaerobic chamber (COY laboratory products, USA) in BHIS medium: 3.7% weight vol^{-1} brain heart infusion (BD, USA) supplemented with 0.5% weight vol^{-1} yeast extract (BD, USA) and 0.1% weight vol^{-1} L-cysteine (Thermo Fisher Scientific, USA); TY medium: 3% weight vol^{-1} trypticase (BD, USA) with 0.5% weight vol^{-1} yeast extract (BD, USA) or 70:30 medium: 6.3% weight vol^{-1} peptone (BD, USA), 0.35% weight vol^{-1} protease peptone (BD, USA), 0.07% weight vol^{-1} ammonium sulfate $(NH_4)_2SO_4$ (Merck USA), 0.106% weight vol^{-1} Tris base (Omnipur, Germany), 1.11% weight vol^{-1} brain heart infusion (BD, USA) and 0.15% weight vol^{-1} yeast extract (BD, USA). To grow strains in plates, 1.5% weight vol^{-1} agar (VWR, USA) was added to medium. Strains used in this work are summarized in Table S1.

Growth assays

C. difficile strains were cultured anaerobically on pre-reduced BHIS broth supplemented with 0.1% sodium taurocholate (NaTC, Sigma, USA) and 0.5% glucose (BHISG + NaTC) for 16 h at 37 ºC to prevent sporulation. Overnight culture was diluted 1:3 with pre-warmed BHISG + NaTC broth and incubated for 2 h at 37 ºC to allow cells to enter exponential phase. Subsequently, culture was diluted 1:100 in fresh BHIS and 100 µL were added to wells in a 96-well plate. Optical density (OD_{600}) was measured every 3 minutes for 22 hours at 37 ºC using Cerillo's Alto^{TM} microplate reader. Three independent biological replicates with four technical replicates each, were performed per sample.

Biofilm formation

Biofilm formation was measured as previously described (18, 19). Briefly, *C. difficile* inoculated BHISG broth was diluted 1:50, 1 mL aliquots were added to 24-well plate and incubated at 37 °C in anaerobic conditions for 24 h. Biofilm biomass was stained with 0.1% crystal violet (CV) for 1h, gently washed with 1X PBS and extracted with 100% ethanol for 2 h at room temperature. Solubilized CV was diluted 1:10 and absorbance was measured at OD_{570} with plate reader (BioTek, Synergy H1).

Spore purification

As previously described (19, 20), 250 µL of a *C. difficile* inoculated BHISF (0.2% Fructose) + NaTC broth was plated on pre-reduced 70:30 agar plates (35 mL) and incubated for 5 days at 37 °C in a COY anaerobic chamber. Sporulating culture was harvested and cleaned with ice-cold sterile Milli-Q water. Nycodenz (Axell USA) 45% solution was used to purified spores by centrifugation at 18,400 × g for 20 min, cellular debris was removed, spore pellet separated and washed with sterile Milli-Q water and stored at −80 °C until use.

Whole genome sequence

C. difficile strains were whole genome sequenced (SeqCenter, USA) and Illumina data was analyzed using Geneious Prime® 2025.1.3. Reads were mapped to *C. difficile* R20291 reference genome (GenBank: CP029423) using Bowtie2 v7.2.2, with default parameters. Whole genome variant calling was performed by Geneious variant finder with a minimum

coverage of five reads and a minimum variant frequency of 0.95 and long INDEL (insertion or deletion) regions were predicted using Find Low/High Coverage tool.

Sporulation assay by ethanol resistance and phase-contrast microscopy

C. difficile sporulation efficiency was assayed as previously described (19, 21). Briefly, plating was performed as previously described in spore purification methods in BHIS, TY and 70:30 agar plates. Cells were harvested after 24 h in 1X PBS, OD_{600} was measured and absorbance of sporulating culture was adjusted to 1. An aliquot of 250 µL was treated with 100% ethanol for 15 minutes at room temperature, serially diluted and spot plated in triplicate onto BHIS + NaTC plates under anaerobic conditions. Sporulation frequency was calculated as the proportion of spores that germinated after ethanol treatment, divided by the total number of CFU in the untreated sample. The ratio of vegetative cells vs spores/sporulating cells was also determined using phase contrast microscopy (Leica DMRX; Germany).

For sporulation timing, cultures were plated in 70:30 plates and incubated at 37 ºC under anaerobic conditions. Samples were harvested after 8, 10, 12, 14, 16, 18, 20 and 24 h into 1 mL 1X PBS. Cells were centrifuged at 18,400 × g for 5 min and fixed with 4% paraformaldehyde. Vegetative and spores/sporulating cells count was determined using phase contrast microscopy (Leica DMRX; Germany).

Transmission electron microscopy (TEM)

As previously described with some modifications (10, 22), spores were fixed overnight with 2.5% glutaraldehyde and 1% paraformaldehyde in 0.1 M cacodylate buffer.

Secondary fixation was performed with 1% osmium tetroxide for 2 h, followed by 30 min staining with 1% tannic acid. Samples were serially dehydrated 30 min each with acetone 30% (with 2% uranyl acetate), 50%, 70%, 90%, and twice with 100% acetone, after which samples were embedded in Spurr resin (22, 23). Thin sections (90 nm) were obtained using a microtome, placed on glow-discharge carbon-coated grids, and double-stained with 2% uranyl acetate followed by lead citrate. Spores were analyzed using a Philips Tecnai 12 Bio Twin microscope at the Unidad de Microscopía Avanzada, Pontificia Universidad Católica de Chile.

Statistical analyses

Statistical significance was determined by Welch's t-test in GraphPad Prism v9.0. <0.05 (*), <0.01 (**), <0.001 (***), <0.0001 (****), ns: no significance. All experiments were performed in triplicate with at least three technical replicates.

Results and discussions

Hyper-sporulating R20291 derivative.

A canonical feature of *C. difficile* spore formation is its asynchronous nature and low yield. By serendipity, in a routine experiment that an isolate of *C. difficile* R20291 (from here on address as $R20291_{CM196}$) presented a marked increase in the number of spores after 24 h incubation in 70:30 sporulation media in comparison with the usual levels obtained in lab with this strain (wild-type strain from here on address as $R20291_{CM210}$) (**Fig. 1A**).

To confirm and evaluate if the increased amounts of spores observed in $R20291_{CM196}$ strain were confined to specific nutritional conditions, a sporulation efficiency assay by ethanol resistance of cells grown in three different media (BHIS, TY and 70:30) widely used in *C. difficile* research was conducted. There was no significant difference in the ethanol-resistant CFU by these two strains when grown in any broth media ($p > 0.05$) (**Fig. 1B,1D and S1**). However, when cells were plated in 70:30 and BHIS agar plates, but no in TY agar plates, a significant difference ($p < 0.01$ and $p < 0.05$, respectively) in ethanol-resistant CFU was observed. This difference was highest in 70:30 agar plates, sporulation efficiency where ~ 92% for the hypersporulating $R20291_{CM196}$ and 3% for the parental $R20291_{CM210}$ strain, respectively (**Fig. 1E, 1G and S2**).

This phenotype was further assessed by phase-contrast microscopy. In 70:30 broth, strain $R20291_{CM196}$ produced 4.9% phase-bright spores, whereas growth on 70:30 agar resulted in a marked increase to 65%. By comparison, $R20291_{CM210}$ displayed substantially lower sporulation frequencies, with 0.2% spores in broth and 4.5% on agar (**Fig. 1C and 1F**). The

higher proportion of ethanol-resistant CFU relative to microscopic counts observed for $R20291_{CM196}$ (92% vs. 65%) likely reflects loss of viability of vegetative cells during sporulation, resulting in their underrepresentation in ethanol-resistance assays but continued detection by microscopy.

$R20291_{CM196}$ exhibits an early onset of sporulation

To determine whether $R20291_{CM196}$ and $R20291_{CM210}$ initiated sporulation at similar times, sporulation-timing assay. Cultures grown on 70:30 agar were harvested at defined intervals was performed and examined by phase-contrast microscopy. Free spores were first detectable in $R20291_{CM196}$ at 12 h, approximately 2 h earlier than in $R20291_{CM210}$, and were ~7-fold more abundant at this time point (7% vs. 1%, respectively) (**Fig. 2A and 2B**). By 14 h, $R20291_{CM196}$ reached 31% spores compared to 1% in $R20291_{CM210}$. After 24 h, more than half of the $R20291_{CM196}$ population consisted of phase-bright spores (57%), representing a ~10-fold higher sporulation level than observed in $R20291_{CM210}$ (5%). These results indicate that $R20291_{CM196}$ not only initiates sporulation earlier but that a larger fraction of the population commits to sporulation over time compared with $R20291_{CM210}$. Because individual cell-transition rates cannot be directly measured under these conditions, the precise rate of sporulation remains undetermined.

Ultrastructural analysis of $R20291_{CM196}$ spores.

To assess whether the hypersporulation phenotype altered spore ultrastructure, transmission electron microscopy was performed. Spores produced by $R20291_{CM196}$ displayed no detectable structural abnormalities and retained characteristic morphological features, including hair-like projections over the electron-dense outer coat (ED-OC) and the lamellar

organization of the coat (Ct) in both thin- and thick-coat morphotypes (**Fig. 2C**). These observations indicate that the hypersporulation phenotype of R20291$_{CM196}$ affects the timing and frequency of sporulation but does not appear to impact spore ultrastructure.

R20291$_{CM196}$ exhibit differences in growth and biofilm formation

To further characterize the physiology of R20291$_{CM196}$, planktonic growth and biofilm formation was examined. R20291$_{CM196}$ exhibited reduced growth, reaching a maximal OD_{600} of 0.1 compared with 0.2 for R20291$_{CM210}$. The onset of the decline phase also occurred earlier in R20291$_{CM196}$, beginning at approximately 10 h post-inoculation, whereas R20291$_{CM210}$ entered decline around 18 h (Fig. 3A). Biofilm formation was significantly diminished in R20291$_{CM196}$, which produced an OD_{570} of 0.3 compared with 0.6 for R20291$_{CM210}$ ($p < 0.0001$) (Fig. 3B). These data suggest that the increased commitment to sporulation observed in R20291$_{CM196}$ may influence both planktonic growth dynamics and the capacity for form sessile communities.

Whole genome sequencing of R20291$_{CM196}$ reveals unique polymorphism.

To determine whether the differences in sporulation commitment in R20291$_{CM196}$ were attributed to underlying genetic variation, R20291$_{CM196}$ and R20291$_{CM210}$ were whole genome sequenced and subjected to comparative genomics against *C. difficile* reference genome CP029423. Both isolates shared five mutations relative to the reference strain. These included two missense mutations: one in *rsbW* (G82V, CDIF27147_00009), which encodes the anti-sigma factor serine protease of SigB, and another in *vncR* (D202G, CDIF27147_02036), a response regulator of a two-component system (Fig. 4A). In addition, two nonsense mutations resulting from single-nucleotide deletions were identified

in *rbsK* (CDIF27147_00429), encoding ribokinase, and in a two-component sensor histidine kinase (CDIF27147_02733) (Fig. 4A); Finally, a single nucleotide insertion in a non-coding intergenic region located 336 bp downstream of CDIF27147_00700 and 144 bp upstream of CDIF27147_00701 was detected (**Fig. 4A**).

Notably, $R20291_{CM196}$ harbors two additional polymorphisms not present in $R20291_{CM210}$. One of these is a missense mutation (L20F) in *rsbV*, which encodes the anti-anti-sigma factor that regulates SigB and plays a crucial role in the general stress response against pH stress, antimicrobial peptides and reactive oxygen species (ROS) (24, 25). In *B. subtilis*, RsbV functions by binding and sequestering RsbW, thereby releasing SigB from the RsbW-SigB complex and allowing for the activation of the SigB regulon (26). Activation of SigB has been shown to reduce sporulation in *B. subtilis* (27), in part through upregulation of *spo0E*, which encodes an aspartyl phosphatase that dephosphorylates the master of sporulation Spo0A (27, 28). In *C. difficile spo0E* mutants exhibit twofold increase in sporulation relative to wild-type, consistent with Spo0E-mediated repression of sporulation observed in *B. subtilis* (16). Because sporulation is an energetically costly process and generally triggered only after other stress-response pathways have been exhausted (29), cells typically activate the general stress response prior to committing to sporulation. The L20F substitution in RsbV may impair its ability to bind RsbW, thereby allowing RsbW to remain associated with SigB. Under this scenario, SigB would remain inhibited, limiting activation of the SigB regulon and its downstream repression of sporulation.

The second mutation unique to $R20291_{CM196}$ is a 2,356 bp deletion encompassing three adjacent genes: a transcriptional regulator (CDIF27147_01521), a pyrroline-5-carboxylate reductase (*proC1*, CDIF27147_01522) involved in the final step of L-proline biosynthesis from glutamate, and the C-terminal 284 bp of an uncharacterized protein (CDIF27147_01523) (**Fig. 4A and 4B**). In *B. subtilis*, only the simultaneous loss of the three pyrroline-5-carboxylate reductases (*proG*, *proH*, and *proI*) results in proline auxotrophy, whereas the individual genes are not essential (30). The *C. difficile* R20291 genome encodes two predicted pyrroline-5-carboxylate reductases, *proC1* and *proC2*(CDIF27147_03465). These proteins share 29–33% identity with *B. subtilis* ProH/ProI and approximately 23% identity with ProG. Thus, deletion of *proC1* alone is unlikely to abolish proline biosynthesis in R20291CM196, as *proC2* remains intact. The deletion also removes CDIF27147_01521, the putative transcriptional regulator, and truncates CDIF27147_01523; however, the functions of these genes remain unknown and are currently under investigation.

FUNDING

This work was supported by 5R01AI177842 from the National Institute of Allergy and Infectious Diseases to D.P-S.

Figure legends

Fig. 1. Hypersporulating *C. difficile* R20291 derivative strain. (A) Phase contrast microscopy of a 24 h sporulating culture. Sporulation efficiency evaluated by ethanol resistant sporulation assay of 24 h sporulating cultures grown in BHIS, TY or 70:30 media (B) broth or (E) agar. Sporulation efficiency evaluated by phase contrast microscopy images of 24 h sporulating cultures grown in BHIS, TY or 70:30 media (C) broth or (F) agar. At least 800 spores/cells were counted from each sample. Representative images of serial spot dilution of ethanol resistant sporulation assay in (D) broth and (G) agar plate. Cells were spotted at 10-fold serial dilutions on BHIS agar plates supplemented with 0.1% sodium taurocholate. ND: no data. Welch's t-test. < 0.05 (*), < 0.01 (**), ns: no significance.

Fig. 2. Early sporulation onset and spore ultrastructure analysis of R20291$_{CM196}$. (**A**) Sporulation timing in 70:30 agar plates. Sporulating culture was monitored at 8, 10, 12, 14, 16, 18, 20 and 24 h. (**B**) Representative phase contrast microscopy images of sporulation timing assay. Numbers on the lower right corner corresponds to the percentage of spores/sporulating cells in the sample at that time. (**C**) Transmission electron microscopy (TEM) of R20291$_{CM196}$ and R20291$_{CM210}$ spores. ED-OC: Electron-dense outer coat. Ct: Coat.

Fig. 3. R20291$_{CM196}$ physiology traits. (**A**) Growth curve of R20291$_{CM196}$ (teal) and R20291$_{CM210}$ (yellow) in BHIS media over 22 h. (**B**) Biofilm formation was evaluated at 24 h by crystal violet staining and measured at OD_{570}. Welch's t-test. < 0.0001 (****)

Fig. 4. Mutations in hypersporulating *C. difficile* R20291$_{CM196}$ strain. (**A**) Description of single nucleotide variants and INDELs present in R20291$_{CM196}$ and R20291$_{CM210}$ strains in comparison with *C. difficile* R20291 reference genome (CP029423). (**B**) Genetic deletion in R20291$_{CM196}$ vs wildtype region in R20291$_{CM210}$.

Fig. S1. Ethanol-resistant cells grow in broth media. Representative images of serial spot dilution of ethanol resistant sporulation assay of R20291$_{CM196}$ and R20291$_{CM210}$. Cells were spotted at 10-fold serial dilutions on BHIS agar plates supplemented with 0.1% sodium taurocholate. U: untreated cells, T: ethanol-treated cells.

Fig. S2. Ethanol-resistant cells grow in agar media. Representative images of serial spot dilution of ethanol resistant sporulation assay of R20291$_{CM196}$ and R20291$_{CM210}$. Cells were spotted at 10-fold serial dilutions on BHIS agar plates supplemented with 0.1% sodium taurocholate. U: untreated cells, T: ethanol-treated cells.

Reference

1. Rupnik M, Wilcox MH, Gerding DN. 2009. Clostridium difficile infection: new developments in epidemiology and pathogenesis. Nat Rev Microbiol 7:526-36.
2. Paredes-Sabja D, Cid-Rojas F, Pizarro-Guajardo M. 2022. Assembly of the exosporium layer in Clostridioides difficile spores. Curr Opin Microbiol 67:102137.
3. Lessa FC, Mu Y, Bamberg WM, Beldavs ZG, Dumyati GK, Dunn JR, Farley MM, Holzbauer SM, Meek JI, Phipps EC, Wilson LE, Winston LG, Cohen JA, Limbago BM, Fridkin SK, Gerding DN, McDonald LC. 2015. Burden of Clostridium difficile infection in the United States. N Engl J Med 372:825-34.
4. Smits WK, Lyras D, Lacy DB, Wilcox MH, Kuijper EJ. 2016. Clostridium difficile infection. Nat Rev Dis Primers 2:16020.
5. McDonald LC, Gerding DN, Johnson S, Bakken JS, Carroll KC, Coffin SE, Dubberke ER, Garey KW, Gould CV, Kelly C, Loo V, Shaklee Sammons J, Sandora TJ, Wilcox MH. 2018. Clinical Practice Guidelines for Clostridium difficile Infection in Adults and Children: 2017 Update by the Infectious Diseases Society of America (IDSA) and Society for Healthcare Epidemiology of America (SHEA). Clin Infect Dis 66:987-994.
6. Kelly CP. 2012. Can we identify patients at high risk of recurrent Clostridium difficile infection? Clin Microbiol Infect 18 Suppl 6:21-7.
7. Paredes-Sabja D, Shen A, Sorg JA. 2014. *Clostridium difficile* spore biology: sporulation, germination, and spore structural proteins. Trends Microbiol 22:406-16.
8. Sorg JA, Sonenshein AL. 2008. Bile salts and glycine as cogerminants for *Clostridium difficile* spores. J Bacteriol 190:2505-12.

9. Deakin LJ, Clare S, Fagan RP, Dawson LF, Pickard DJ, West MR, Wren BW, Fairweather NF, Dougan G, Lawley TD. 2012. The *Clostridium difficile spo0A* gene is a persistence and transmission factor. Infect Immun 80:2704-11.

10. Castro-Córdova P, Mora-Uribe P, Reyes-Ramírez R, Cofré-Araneda G, Orozco-Aguilar J, Brito-Silva C, Mendoza-León MJ, Kuehne SA, Minton NP, Pizarro-Guajardo M, Paredes-Sabja D. 2021. Entry of spores into intestinal epithelial cells contributes to recurrence of Clostridioides difficile infection. Nat Commun 12:1140.

11. Dembek M, Willing SE, Hong HA, Hosseini S, Salgado PS, Cutting SM. 2017. Inducible Expression of *spo0A* as a Universal Tool for Studying Sporulation in *Clostridium difficile*. Front Microbiol 8:1793.

12. Fimlaid KA, Bond JP, Schutz KC, Putnam EE, Leung JM, Lawley TD, Shen A. 2013. Global analysis of the sporulation pathway of *Clostridium difficile*. PLoS Genet 9:e1003660.

13. Saujet L, Pereira FC, Serrano M, Soutourina O, Monot M, Shelyakin PV, Gelfand MS, Dupuy B, Henriques AO, Martin-Verstraete I. 2013. Genome-wide analysis of cell type-specific gene transcription during spore formation in *Clostridium difficile*. PLoS Genet 9:e1003756.

14. Underwood S, Guan S, Vijayasubhash V, Baines SD, Graham L, Lewis RJ, Wilcox MH, Stephenson K. 2009. Characterization of the sporulation initiation pathway of *Clostridium difficile* and its role in toxin production. J Bacteriol 191:7296-305.

15. Pereira FC, Saujet L, Tome AR, Serrano M, Monot M, Couture-Tosi E, Martin-Verstraete I, Dupuy B, Henriques AO. 2013. The spore differentiation pathway in the enteric pathogen *Clostridium difficile*. PLoS Genet 9:e1003782.

16. DiCandia MA, Edwards AN, Alcaraz YB, Monteiro MP, Lee CD, Vargas Cuebas G, Bagchi P, McBride SM. 2024. A conserved switch controls virulence, sporulation, and motility in C. difficile. PLoS Pathog 20:e1012224.

17. Edwards AN, Anjuwon-Foster BR, McBride SM. 2019. RstA Is a Major Regulator of Clostridioides difficile Toxin Production and Motility. mBio 10.

18. Reyes Ruiz LM, King KA, Agosto-Burgos C, Gamez IS, Gadda NC, Garrett EM, Tamayo R. 2022. Coordinated modulation of multiple processes through phase variation of a c-di-GMP phosphodiesterase in Clostridioides difficile. PLoS Pathog 18:e1010677.

19. Cid-Rojas F, Guerrero-Araya E, Brito-Silva C, Pizarro-Guajardo M, Rodríguez-Sanchéz C, Paredes-Sabja D. 2025. Phylogenomic analysis of the collagen-like BclA proteins in Clostridioides difficile. bioRxiv:2025.06.24.661383.

20. Edwards AN, McBride SM. 2016. Isolating and Purifying Clostridium difficile Spores. Methods Mol Biol 1476:117-28.

21. Edwards AN, McBride SM. 2017. Determination of the in vitro Sporulation Frequency of Clostridium difficile. Bio Protoc 7.

22. Pizarro-Guajardo M, Calderón P, Romero-Rodriguez A, Paredes-Sabja D. 2020. Characterization of exosporium layer variability of *Clostridioides difficile* spores in the epidemically relevant strain R20291. Front Microbiol 11:1345.

23. Paredes-Sabja D, Cofre-Araneda G, Brito-Silva C, Pizarro-Guajardo M, Sarker MR. 2012. *Clostridium difficile* spore-macrophage interactions: spore survival. PLoS One 7:e43635.

24. Hecker M, Pané-Farré J, Völker U. 2007. SigB-dependent general stress response in Bacillus subtilis and related gram-positive bacteria. Annu Rev Microbiol 61:215-36.

25. Kint N, Janoir C, Monot M, Hoys S, Soutourina O, Dupuy B, Martin-Verstraete I. 2017. The alternative sigma factor σ(B) plays a crucial role in adaptive strategies of Clostridium difficile during gut infection. Environ Microbiol 19:1933-1958.

26. Brigulla M, Hoffmann T, Krisp A, Völker A, Bremer E, Völker U. 2003. Chill induction of the SigB-dependent general stress response in Bacillus subtilis and its contribution to low-temperature adaptation. J Bacteriol 185:4305-14.

27. Reder A, Albrecht D, Gerth U, Hecker M. 2012. Cross-talk between the general stress response and sporulation initiation in Bacillus subtilis - the σ(B) promoter of spo0E represents an AND-gate. Environ Microbiol 14:2741-56.

28. Reder A, Gerth U, Hecker M. 2012. Integration of σB activity into the decision-making process of sporulation initiation in Bacillus subtilis. J Bacteriol 194:1065-74.

29. Kint N, Morvan C, Martin-Verstraete I. 2022. Oxygen response and tolerance mechanisms in Clostridioides difficile. Curr Opin Microbiol 65:175-182.

30. Belitsky BR, Brill J, Bremer E, Sonenshein AL. 2001. Multiple genes for the last step of proline biosynthesis in Bacillus subtilis. J Bacteriol 183:4389-92.

Figure 1

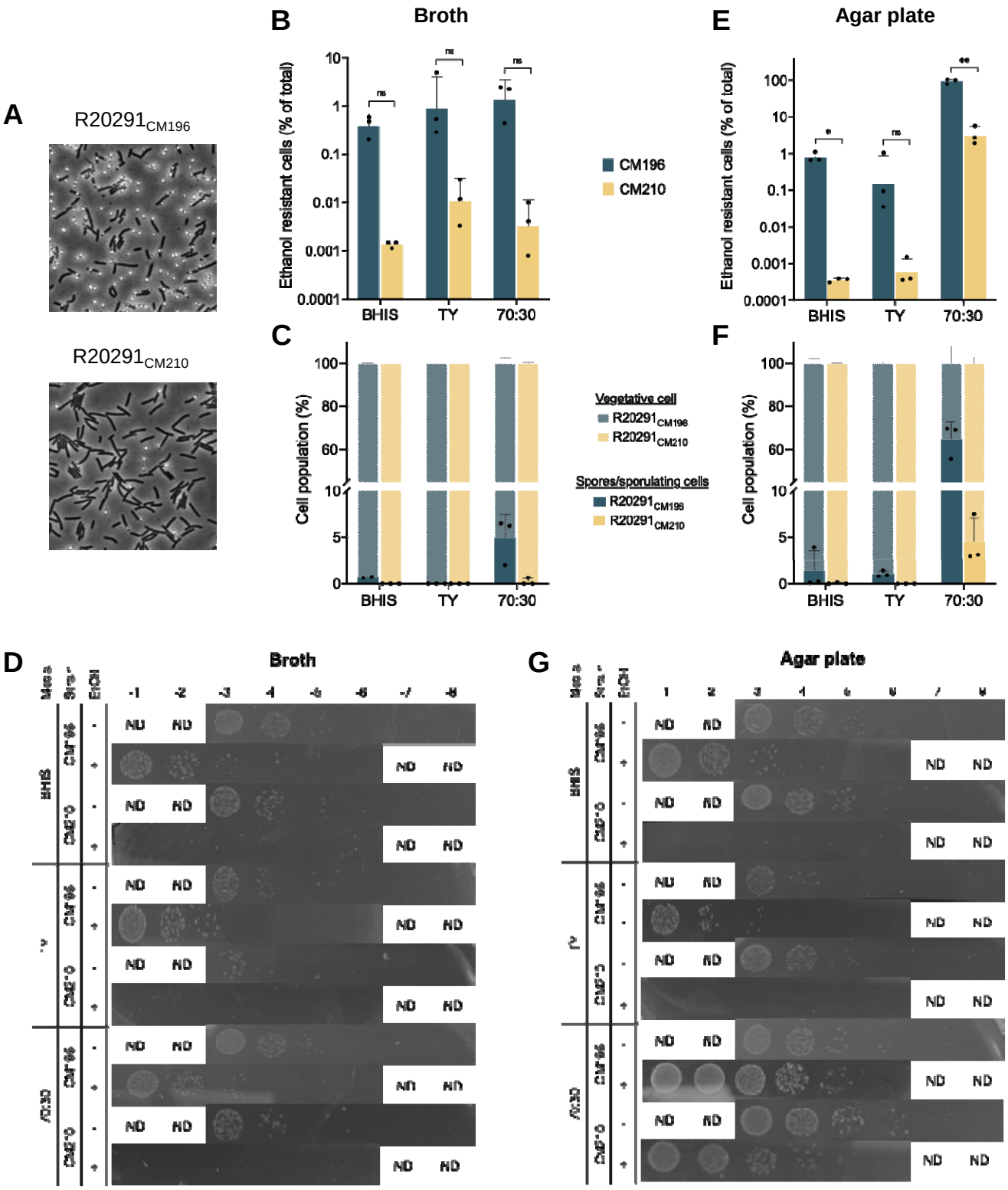
A
R20291CM196
R20291CM210
B
Broth
Ethanol resistant cells (% of total)
BHIS
TY
70:30
CM196
CM210
E
Agar plate
C
Cell population (%)
Vegetative cell
R20291CM196
R20291CM210
Spores/sporulating cells
F
D
Broth
G
Agar plate
ND

Figure 2

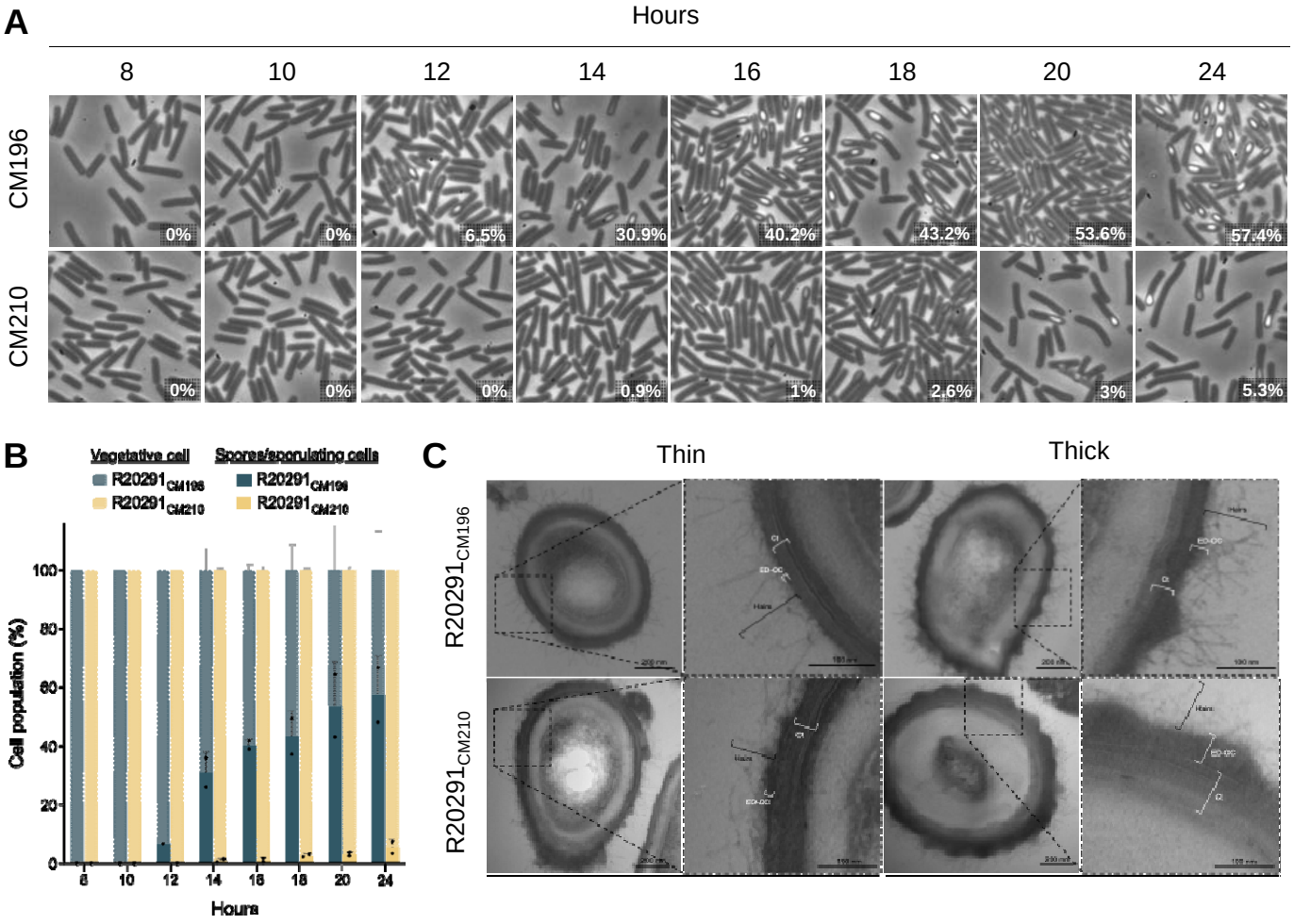
A
Hours
8
10
12
14
16
18
20
24
CM196
CM210
0%
0%
6.5%
30.9%
40.2%
43.2%
53.6%
57.4%
0%
0%
0%
0.9%
1%
2.6%
3%
5.3%
B
Vegetative cell
Spores/sporulating cells
R20291CM196
R20291CM210
R20291CM196
R20291CM210
Cell population (%)
Hours
C
Thin
Thick
R20291CM196
R20291CM210

Figure 3

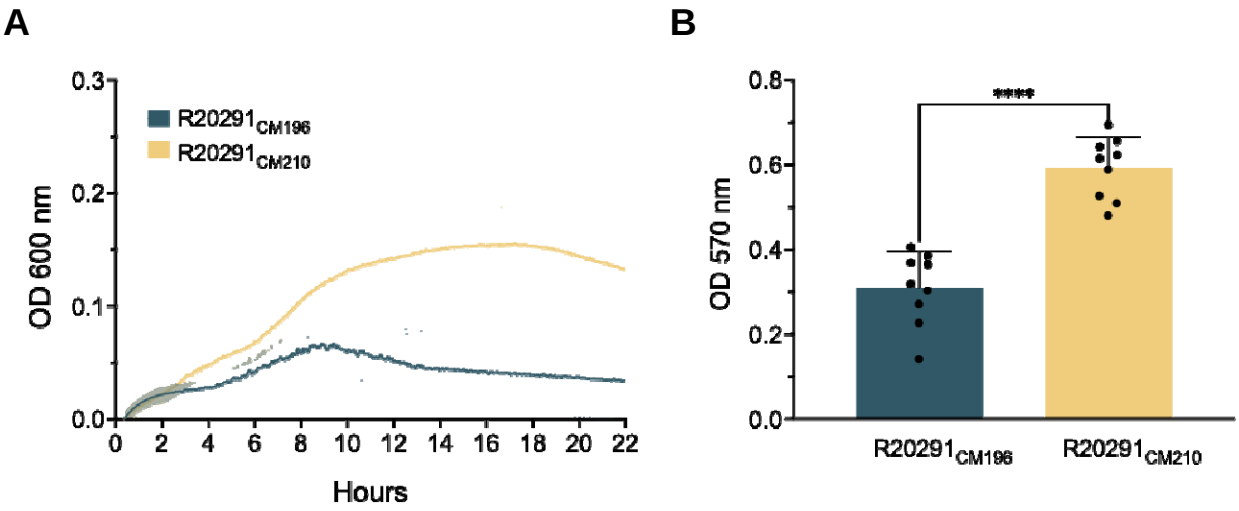
A
B
OD 600 nm
Hours
R20291CM196
R20291CM210
OD 570 nm
****
R20291CM196
R20291CM210

Figure 4

A

locus_tag	Gene name	Description	Genome position (pb)	Polymorphism type	Mutation	nucleotide change	Amino acid change	Coverage	Variant frequency (%)	Genomes	
										CM196	CM210
Coding region polymorphisms											
CDIF27147_00009	*rsbV*	anti-sigma-B factor antagonist	9,166	SNV	Missense	C -> T	L20F	213	99.5	X	-
CDIF27147_00010	*rsbW*	serine-protaine kinase	9,894	SNV	Missense	G -> T	G82V	189	99.7	X	X
CDIF27147_00429	*rbsK*	ribokinase	371,826	Deletion	Nonsense	(A)5 -> (A)4	V55=fs*2	165	95.3	X	X
CDIF27147_02036	*vncR*	two-component system response regulator	2,134,234	SNV	Missense	A -> G	D202G	173	100	X	X
CDIF27147_02733	-	two-component sensor histidine kinase	2,895,029	Deletion	Nonsense	(T)7 -> (T)6	K438=fs*12	162	96.2	X	X
Non-coding region polymorphisms											
-	-	-	665626	Insertion	-	(A)5 -> (A)6	-	177	96.9	X	X
-	-	-	2090870	Deletion	-	- C	-	281	97.9	-	X
INDEL											
CDIF27147_01521	-	Transcriptional regulator	1,602,931 - 1,605,267	Deletion	-	-	-	-	100	X	-
CDIF27147_01522	*proC1*	pyrroline-5-carboxylate reductase									
CDIF27147_01523	-	Uncharacterized protein									

fs: frame shift

*: Stop codon. Number after "=" denotes new stop codon position after indel event.
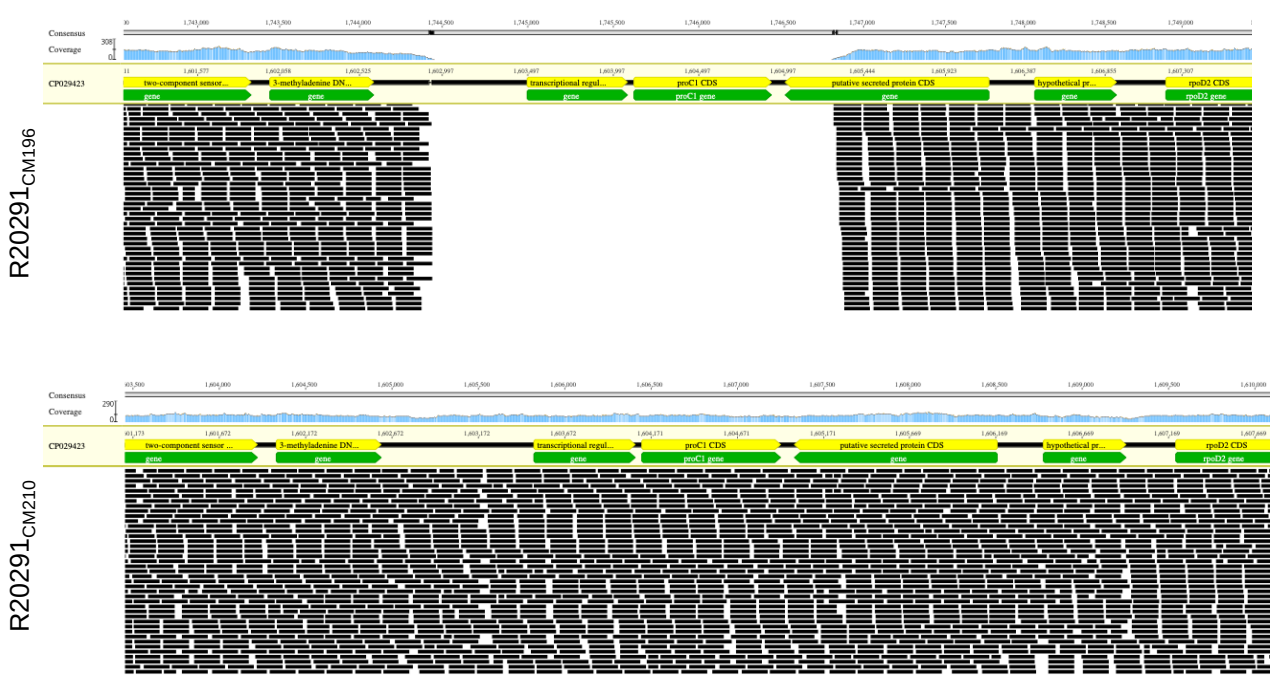
B